J. Fluid Mech. (1980), *vol.* 100, *part* 4, *pp.* 739–767
Printed in Great Britain

Gravity currents entering a two-layer fluid

By JUDITH Y. HOLYER† AND HERBERT E. HUPPERT

Department of Applied Mathematics and Theoretical Physics, University of Cambridge

(Received 5 June 1978 and in revised form 12 February 1980)

This paper presents a study of steady gravity currents entering a two-layer system, with the current travelling either along the boundary to form a boundary current, or between the two different layers to form an intrusion. It is shown that, at the front of an intrusion, the streamlines meet at angles of 120° at a stagnation point. For an energy-conserving current the volume inflow rate to the current, the velocity of propagation and the downstream depths are determined. In contrast to the pioneering study of Benjamin (1968), it is found that the depth of the current is not always uniquely determined and it is necessary to use some principle additional to the conservation relationships to determine which solution occurs. An appropriate principle is obtained by considering dissipative currents. In general, if the volume inflow rate to a current is prescribed, the current loses energy in order to maintain a momentum balance. We thus suggest the criterion that the energy dissipation is a maximum for a fixed volume inflow rate. It is postulated that the energy which is lost will go to form a stationary wave train behind the current. A nonlinear calculation is carried out to determine the amplitude and wavelength of these waves for intrusions. Such waves have been observed on intrusions in laboratory experiments and the results of the calculation are found to agree well with the experiments. Similar waves have not been observed on boundary currents because the resulting waves have too much energy and break.

1. Introduction

A gravity current is formed whenever one fluid flows primarily horizontally into a lighter or heavier fluid. When the flow is into a two-layer fluid, the gravity current may be sufficiently heavy to travel along the bottom or sufficiently light to travel along the top, to form a boundary gravity current. Alternatively, when the current is of a density between the densities of the upper and lower layers, the current will travel at the intermediate height to form an intermediate gravity current, or intrusion. There are many naturally occurring examples of gravity currents and intrusions, including cold fronts and sea-breeze fronts, the currents that form when freshwater rivers flow into salt-water oceans and when freshwater locks empty into the sea, thunderstorm outflows and avalanches of snow-laden air.

The classical theoretical work on the subject (Benjamin 1968) considers gravity currents entering homogeneous fluid using perfect-fluid theory, though including a

† Present address: Topexpress, Ltd. 1 Portugal Place, Cambridge.

0022–1120/80/4582–1780 $02.00

model for energy dissipation. The work presented here extends Benjamin's work to currents of prescribed volume flux entering a two-layer fluid as either a boundary current or an intrusion. This two-layer model is studied as a preliminary to investigating a continuously stratified model in the future. It is found that, except for specific volume inflow rates, energy cannot be conserved between upstream and downstream sections. In contrast to Benjamin's work, we find that the depth of the current is not always uniquely determined and it is necessary to use some further condition to determine which solution will occur. The condition suggested is that the energy dissipation is a maximum for a fixed volume inflow rate to the current. This is equivalent to the suggestion that the total energy of the current falls to its lowest possible value. This is discussed further in § 4. The stability of the current is considered in § 5. In order to keep the model as simple as possible, we consider the different density fluids to be immiscible and to have surface tension forces acting along the interfaces between them. Surface-tension forces play an important role in an investigation of the stability of the steady solution, but only a marginal role in the determination of the steady solution itself. For this reason we neglect surface tension effects which stabilize short-wavelength disturbances, until § 5, where we consider the stability of the current. In § 6, we examine the consequence of allowing the energy which is lost by most currents to form a stationary wave train behind the current. A nonlinear calculation is carried out to determine the amplitudes and wavelengths of these waves for intrusions. Such waves have been observed on intrusions in laboratory experiments conducted at DAMTP by Mr J. E. Simpson, and the results of our calculations are found to agree well with the experiments. Similar waves have not been observed on boundary gravity currents and we believe this to be because the wave train would consist of waves so high that they would break.

Experimental work in the field of gravity currents has mostly been concerned with the flow of salt water into fresh water, as a boundary current, using a lock exchange (Keulegan 1958; Simpson 1969). Work has also been carried out on the emptying of a cavity, which, apart from differences in the stability of the system, is equivalent to a bottom boundary current (Zukovski 1966; Gardner & Crow 1970). The work on emptying cavities has shown that it is possible to obtain energy-conserving gravity currents experimentally. Both Zukovski and Gardner & Crow obtained supercritical flows close to Benjamin's half-depth energy-conserving solution. For the emptying cavity, this solution is stable to Kelvin–Helmholtz waves, and hence can be obtained. For the bottom boundary current, Benjamin's half-depth solution is unstable (Benjamin 1968, § 4.1). Thus Keulegan and Simpson do not observe the half-depth energy-conserving solution, but always see large-amplitude billows downstream. Recent experiments by Britter & Simpson (1978, see figure 1, plate 1), which were designed to be as close as possible to Benjamin's theoretical model, clearly show Kelvin–Helmholtz billows on a bottom boundary current. We thus see that it will be very important to know, in any given physical situation, whether or not the current is unstable to Kelvin–Helmholtz waves.

2. Energy-conserving currents and infinite-depth solutions

We consider the problems of a boundary current and an intrusion entering a two-layer fluid. For given layer densities and upstream fluid depths, the mass, momentum and energy conservation equations are obtained. These equations are then manipulated to obtain two coupled polynomial equations for the downstream depths. These equations are solved numerically in § 3. In this section we consider various special cases, including the case of currents entering infinitely deep stratified fluids. For a boundary current entering an infinitely deep homogeneous fluid, Benjamin (1968) showed that no energy-conserving solution could exist. We show here, however, that the introduction of two-layer stratification makes it possible to maintain a current without energy loss.

In § 2.2, we consider the flow locally in the neighbourhood of the most forward point of the intrusion. By doing a calculation similar to that resulting in the 120° angle for surface waves (Stokes 1880), it is shown that the furthest forward point of the intrusion is a stagnation point and that each angle at the front must be 120°.

We concentrate entirely on steady flows, which are considered to be the response when there no longer remain any transients due to the initiation of the current. The gravity current disturbance then generates only a stationary wave pattern. The dispersion relationship for the two-layer system upstream (Phillips 1977 (5.3.6)) indicates that the group velocity of waves on the interface is always less than the phase velocity evaluated at the same wavelength. This implies that energy is carried downstream from the steadily propagating current and does not appear upstream, as explained for an analogous flow so evocatively by Lighthill (§ 3.9, 1978).

2.1. *The boundary current*

The model is shown in figure 2. The current is brought to rest by imposing on the system a velocity equal and opposite to the velocity of the current. The velocity is assumed to be uniform and horizontal across upstream and downstream sections far from the current head, O, which implies that the pressure is hydrostatic across these sections. The possibility of having waves on the downstream interfaces is considered in § 6. The fluids are taken to be inviscid, incompressible and irrotational with zero surface tension (and no diffusion) between the fluids.

We choose units so that $d_1 = 1$ and we write

$$\alpha_{12} = (\rho_1 - \rho_2)/\rho_2, \quad \alpha_{23} = (\rho_2 - \rho_3)/\rho_3$$

and

$$\alpha_{13} = (\rho_1 - \rho_3)/\rho_3 = \alpha_{12}(1 + \alpha_{23}) + \alpha_{23}.$$

We choose the zero pressure level so that $p = 0$ at O. As the current is at rest, Bernoulli's theorem implies $p = 0$ downstream on the floor. There will be a stagnation point at O and the angle made by the interface with the floor will be 60°. The proof of this was given by von Kármán (1940) for a current entering a homogeneous fluid and it also applies here. We suppose the depths $d_1 (= 1)$ and Z and the densities ρ_1, ρ_2 and ρ_3 are specified and we seek the velocities c_1, c_2 and c_3, the upstream pressure on the

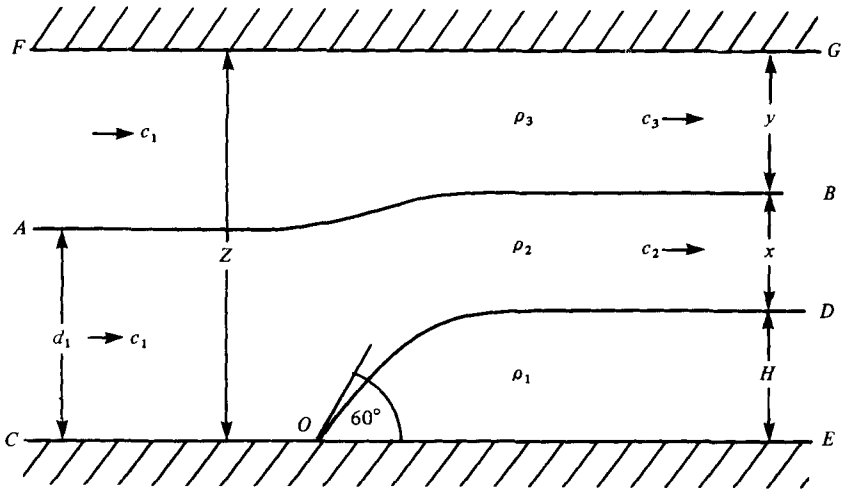

FIGURE 2. A boundary current.

lower boundary, p_2, and the depths x and H. We use mass continuity, Bernoulli's equation along each streamline and the momentum integral.

Mass continuity gives

$$c_1 = c_2 x \quad \text{and} \quad c_1(Z-1) = c_3 y. \tag{2.1), (2.2}$$

Bernoulli's equation on OD gives

$$c_2^2 = 2\alpha_{12} g H. \tag{2.3}$$

From OC we find that

$$p_2 = -\tfrac{1}{2}\rho_2 c_1^2. \tag{2.4}$$

By applying Bernoulli's equation along AB in the ρ_3-fluid, we find

$$p_2/\rho_3 = \alpha_{23} g(1-x) - \alpha_{13} g H + \tfrac{1}{2}(c_3^2 - c_1^2). \tag{2.5}$$

Conservation of momentum flux in $FGEC$ then gives

$$\begin{aligned}\rho_2 c_1^2 - \rho_2 c_2^2 x + \rho_3 c_1^2(Z-1) - \rho_3 c_3^2 y + p_2 Z - \tfrac{1}{2}\rho_2 g - \tfrac{1}{2}\rho_3 g(Z-1)^2 - \rho_2 g(Z-1) \\ = -\tfrac{1}{2}\rho_1 g H^2 - \rho_1 g H x - \tfrac{1}{2}\rho_2 g x^2 - \rho_1 g H Z - \rho_2 g x Z \\ + (\rho_1 g H + \rho_2 g x)(x+H) - \tfrac{1}{2}\rho_3 g y^2.\end{aligned} \tag{2.6}$$

Equations (2.1)–(2.6) are six independent equations in six unknowns. By eliminating p_2 from (2.4) and (2.5) and using mass continuity, we find that

$$c_3^2 = \frac{2g(Z-1)^2[\alpha_{13}H - \alpha_{23}(1-x)]}{(Z-1)^2 + \alpha_{23} y^2}. \tag{2.7}$$

Substituting for p_2 in (2.6) and using (2.3) and (2.7) to eliminate c_2^2 and c_3^2, we obtain an equation in x and H only:

$$\begin{aligned}2[2(Z-1) - y + \alpha_{23} y] \frac{[\alpha_{13}H - \alpha_{23}(1-x)](Z-1)y}{(Z-1)^2 + \alpha_{23} y^2} + 2\alpha_{12}(1+\alpha_{23}) H x(2-x) \\ = \alpha_{12}(1+\alpha_{23}) H(2Z-H) + \alpha_{23}[(Z-1)^2 - y^2].\end{aligned} \tag{2.8}$$

The second equation for x and H comes from (2.2). Substituting for c_2^2 and c_3^2 from (2.3) and (2.7) and using (2.1), we obtain

$$\frac{[\alpha_{13}H-\alpha_{23}(1-x)]\,y^2}{(Z-1)^2+\alpha_{23}y^2} = \alpha_{12}Hx^2. \tag{2.9}$$

Equations (2.8) and (2.9) have been solved numerically for certain values of the free parameters Z, α_{12} and α_{23} and these solutions are discussed in § 3. First we look at some special cases.

(i) $\rho_2 = \rho_3$

If $\rho_2 = \rho_3$ the current is entering a homogeneous medium, which is the problem considered by Benjamin (1968). In this case $\alpha_{23} = 0$ and the only non-trivial (i.e. $H \neq 0$) solution of (2.8) and (2.9) is $H = \frac{1}{2}Z$, $x = \frac{1}{2}$ and $c_2 = c_3$, which is in agreement with Benjamin's unique energy-conserving solution.

(ii) $\rho_3 = 0$

If $\rho_3 = 0$ we have the problem of flow beneath a free surface and we find that

$$1-2x+\alpha_{12}(1-x)^2(1-x^2) = 0, \quad H[1+\alpha_{12}(1-x^2)] = 1-x. \tag{2.10}$$

For small α_{12}, these give $x = \frac{1}{2}(1+\frac{3}{16}\alpha_{12})$ and $H = \frac{1}{2}(1-\frac{15}{16}\alpha_{12})$, which agrees with Benjamin (1968, p. 211).

(iii) $Z \gg 1$

An interesting case to examine is that of $Z \to \infty$ with x and H finite, which we can solve exactly. If $\rho_2 = \rho_3$, the model reverts to that considered by Benjamin (1968), and in this limit no current can exist as the momentum fluxes cannot be balanced unless a wake is introduced behind the current head. However, if $\rho_2 \neq \rho_3$, the existence of two layers makes it possible to balance the momentum by the change in velocity as the layer passes over the current.

We let $Z \to \infty$ in (2.8) and (2.9). In this limit (2.9) gives

$$H[1+\gamma(1-x^2)] = 1-x, \tag{2.11}$$

where

$$\gamma = \frac{\alpha_{12}}{\alpha_{23}}(1+\alpha_{23}) = \frac{\rho_1-\rho_2}{\rho_2-\rho_3}.$$

Substituting this value for H in (2.8) gives

$$1-2x+\gamma(1-x^2)(1-x)^2 = 0, \tag{2.12}$$

which is of the same form as (2.10). The solution for x and H for different values of γ is shown in figure 3, which indicates that (2.12) always has a solution with $\frac{1}{2} \leqslant x \leqslant 1$. If γ is infinite, and hence $\rho_2 = \rho_3$, then $x = 1$ and $H = 0$ and no current can be maintained. However, if $\gamma = 0$, and hence $\rho_1 = \rho_2$, then $x = H = \frac{1}{2}$. From figure 3 we see that in an infinite-depth fluid it is possible to maintain an energy-conserving current for all finite values of γ.

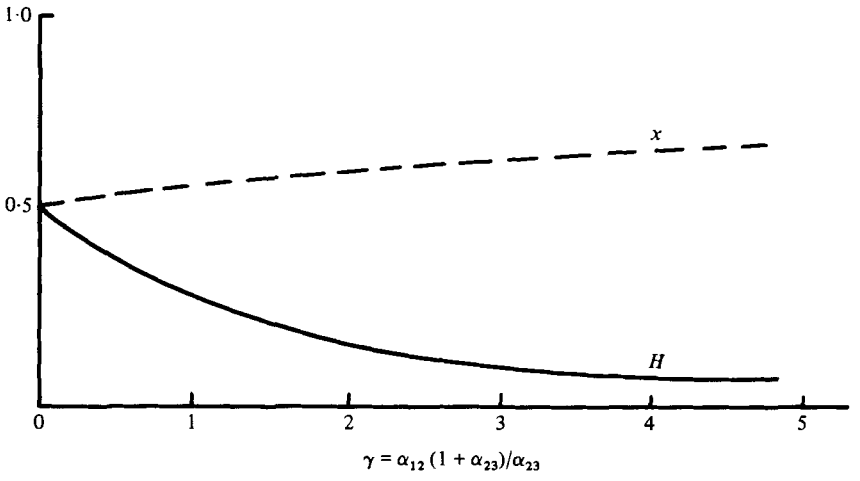

FIGURE 3. The energy-conserving solution for the boundary current when $Z \gg 1$.

2.2. *The local solution at the front of the intrusion*

The model for the intrusion is shown in figure 4. As for the boundary current, we assume that the fluids are inviscid and incompressible, and we neglect any surface-tension effects. We again work in the frame in which the current is at rest. We first show that the point, O, where the three dividing streamlines meet is a stagnation point.

Suppose O is not a stagnation point and that the speed of each fluid at O is V_1, V_2 and V_3 in the ρ_1, ρ_2 and ρ_3 fluids respectively. We have assumed that the current is at rest and hence that V_1 is zero. If V_2 and V_3 were both non-zero then we would require two smooth streamlines to merge smoothly at O. This cannot occur, for the same reason that streamlines always meet a boundary at a non-zero angle. Thus only one of V_2 and V_3 can be non-zero. If we apply continuity of pressure across the streamlines at O and use Bernoulli's equation, we find that

$$\rho_1 gX = \rho_2(\tfrac{1}{2}V_2^2 + gX) = \rho_3(\tfrac{1}{2}V_3^2 + gX),$$

where X is the reference height of O. From this the only consistent solution with $V_j = 0$, where $j = 2$ or 3, is

$$g(\rho_j - \rho_1)X = 0.$$

So $X = 0$ and hence the third velocity is also zero.

Thus O is a stagnation point, and the dividing streamlines can be taken locally as straight lines meeting at non-zero angles, as shown in figure 5. In region i the velocity potential will be

$$\phi_i = r^{n_i}(A_i \cos n_i\theta + B_i \sin n_i\theta).$$

The boundary conditions of no normal velocity on the streamlines OA, OB and OC imply that

$$n_1(\psi + \chi) = \pi, \quad n_2(\pi - \beta - \psi) = \pi \quad \text{and} \quad n_3(\pi + \beta - \chi) = \pi. \tag{2.13}$$

These three equations are not independent and for a solution to exist

$$\pi(n_1^{-1} + n_2^{-1} + n_3^{-1}) = 2\pi. \tag{2.14}$$

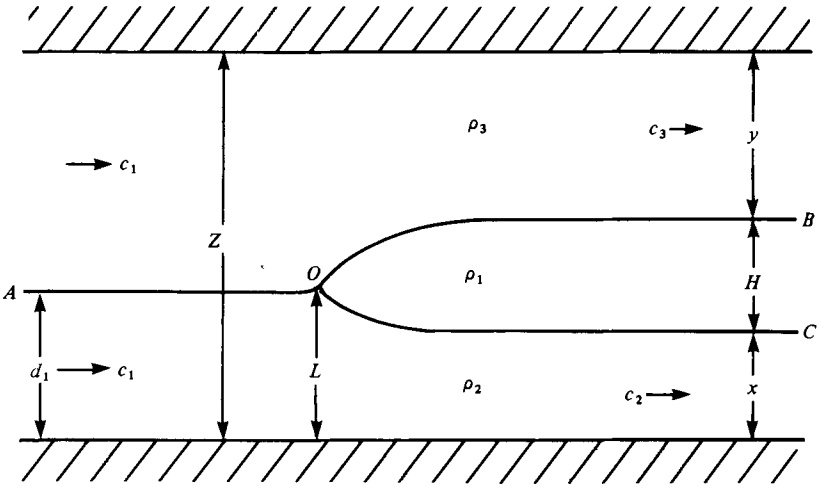

FIGURE 4. An intrusion.

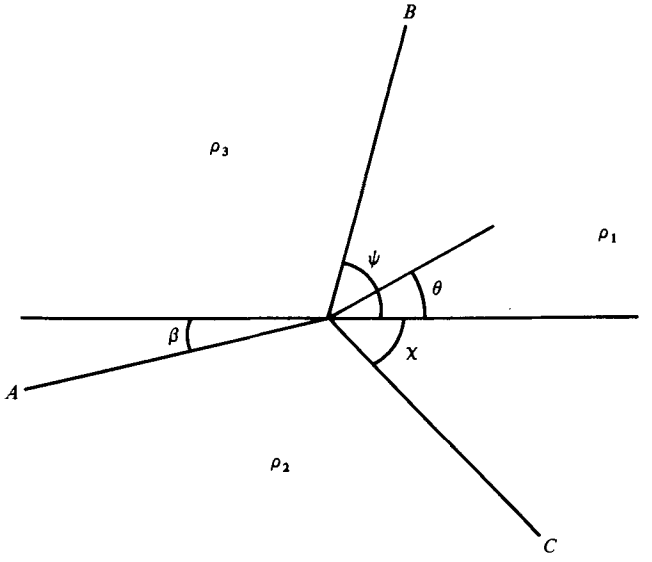

FIGURE 5. The stagnation point at the front of the intrusion.

The other boundary conditions we must apply are continuity of pressure across dividing streamlines. Choosing the pressure to be zero at O and using continuity of pressure across OA and Bernoulli's theorem, we find that

$$p_2(\tfrac{1}{2}|\nabla\phi_2|^2 - gr\sin\beta) = \rho_3(\tfrac{1}{2}|\nabla\phi_3|^2 - gr\sin\beta).$$

Substituting for $|\nabla\phi_2|^2$ and $|\nabla\phi_3|^2$, we obtain

$$\rho_2 n_2^2 r^{2(n_2-1)}(A_2^2 + B_2^2) - \rho_3 n_3^2 r^{2(n_3-1)}(A_3^2 + B_3^2) = 2(\rho_2 - \rho_3) gr\sin\beta. \tag{2.15}$$

Similarly, continuity of pressure across OB and OC gives

$$\rho_3 n_3^2 r^{2(n_3-1)}(A_3^2+B_3^2)-\rho_1 n_1^2 r^{2(n_1-1)}(A_1^2+B_1^2) = 2(\rho_1-\rho_3)gr\sin\psi \tag{2.16}$$

and

$$\rho_2 n_2^2 r^{2(n_2-1)}(A_2^2+B_2^2)-\rho_1 n_1^2 r^{2(n_1-1)}(A_1^2+B_1^2) = 2(\rho_2-\rho_1)gr\sin\chi. \tag{2.17}$$

Each of these equations must be true for all r, hence $2(n_i-1) = 1, i = 1, 2, 3$. From this we see that $n_1 = n_2 = n_3 = \frac{3}{2}$. Putting this result into (2.3), we obtain

$$\psi+\chi = \tfrac{2}{3}\pi, \quad \pi-\beta-\psi = \tfrac{2}{3}\pi, \quad \pi+\beta-\chi = \tfrac{2}{3}\pi. \tag{2.18}$$

Hence the angle between each pair of streamlines is 120°.

Equations (2.15)–(2.17) are not independent and for consistency they require

$$(\rho_2-\rho_3)\sin\beta+(\rho_1-\rho_3)\sin\psi = (\rho_2-\rho_1)\sin\chi. \tag{2.19}$$

Substituting for ψ and β in (2.19), we obtain

$$\tan\chi = \frac{\rho_1+\rho_2-2\rho_3}{\sqrt{3}(\rho_2-\rho_1)}. \tag{2.20}$$

Suppose that $\rho_2 > \rho_1 > \rho_3$ so that the intrusion is of density ρ_1. Then, from (2.20), we see that $\tan\chi > 3^{-\frac{1}{2}}$, and hence $\pi/6 < \chi < \pi/2$. Thus, since $\chi < \pi/2$ and $\psi < \pi/2$, the point O will always be at the front of the intrusion.

Also we find, from (2.18) and (2.20), that

$$\tan\beta = \frac{\rho_2+\rho_3-2\rho_1}{\sqrt{3}(\rho_2-\rho_3)}. \tag{2.21}$$

From (2.21) we see that β will be negative, and hence that the streamline will be above the horizontal, if $\rho_1 > \frac{1}{2}(\rho_2+\rho_3)$ and that β will be positive if $\rho_1 < \frac{1}{2}(\rho_2+\rho_3)$. Thus if the intrusion is of larger density than the average it will 'sink' and $\beta < 0$, while if the density of the intrusion is less than the average it will 'rise'. This effect can be seen in figure 12 (plate 1), where the density of the intrusion is larger than the average and the 120° system of angles is tilted so that $\beta < 0$. In figure 13 (plate 2) the intrusion is of a slightly larger density than the average. Here we can again see that the intrusion has 'sunk' and $\beta < 0$. In figure 14 (plate 2) the intrusion is lighter than the average density and the 120° system of angles is tilted so that $\beta > 0$.

2.3. *The intrusion*

We now obtain the governing equations for the intrusion. We choose units so that $d_1 = 1$ and write

$$\alpha'_{21} = (\rho_2-\rho_1)/\rho_2, \quad \alpha'_{13} = (\rho_1-\rho_3)/\rho_3$$

and

$$\alpha'_{23} = (\rho_2-\rho_3)/\rho_3 = (\alpha'_{21}+\alpha'_{13})/(1-\alpha'_{21}).$$

The zero pressure level is chosen so that $p = 0$ at O. The upstream pressure on the central interface is p_2. Applying Bernoulli's equation on OA in the ρ_2- and ρ_3-fluids respectively, we obtain

$$p_2+\tfrac{1}{2}\rho_2 c_1^2 = \rho_2 g(L-1) \tag{2.22}$$

and

$$p_2+\tfrac{1}{2}\rho_3 c_1^2 = \rho_3 g(L-1). \tag{2.23}$$

Now $\rho_2 \neq \rho_3$, so $p_2 = 0$ and

$$L = 1 + \tfrac{1}{2}\frac{c_1^2}{g}. \tag{2.24}$$

Thus the stagnation point O is raised above the interface far upstream to enable the pressure to be continuous across the upstream interface. Mass continuity gives

$$c_1 = c_2 x \quad \text{and} \quad c_1(Z-1) = c_3 y. \tag{2.25}$$

Bernoulli's equation on OC gives

$$c_2^2(1-\alpha'_{21}x^2) = 2\alpha'_{21}g(1-x). \tag{2.26}$$

Bernoulli's equation on OB gives

$$c_3^2\left(1+\frac{\alpha'_{13}y^2}{(Z-1)^2}\right) = 2\alpha'_{13}g(Z-1-y). \tag{2.27}$$

Conservation of momentum over the entire region then gives

$$\begin{aligned}-\rho_2 c_2^2 x(1-x) - \rho_3 c_3^2 y(Z-1-y)/(Z-1) = {} & -\tfrac{1}{2}\rho_2 g d_1^2 + \tfrac{1}{2}\rho_3 g(Z-1)^2 \\ & -\tfrac{1}{2}\rho_1 g x^2 + \tfrac{1}{2}\rho_1 g y^2 - \tfrac{1}{2}\rho_1 g Z(Z-2L) + \tfrac{1}{2}\rho_2 g x^2 - \tfrac{1}{2}\rho_3 g y^2. \end{aligned} \tag{2.28}$$

Substituting for c_2^2 and c_3^2 from (2.26) and (2.27) in the momentum equation yields

$$\begin{aligned} 2\alpha'_{21}\frac{(1+\alpha'_{13})}{(1-\alpha'_{21})}x(1-x)\frac{(2-x-\alpha'_{21}x)}{(1-\alpha'_{21}x^2)} & \\ + 2\alpha'_{13}y(Z-1-y)\frac{[2(Z-1)-y+\alpha'_{13}y]}{(Z-1)^2+\alpha'_{13}y^2}(Z-1) & \\ = \alpha'_{21}\frac{(1+\alpha'_{13})}{(1-\alpha'_{21})}(1-x^2) + \alpha'_{13}[(Z-1)^2-y^2]. & \end{aligned} \tag{2.29}$$

From (2.26) and (2.27) and mass continuity, we find that

$$\alpha'_{21}(1-x)x^2/(1-\alpha'_{21}x^2) = \alpha'_{13}(Z-1-y)y^2/[(Z-1)^2+\alpha'_{13}y^2]. \tag{2.30}$$

Equations (2.29) and (2.30) are two independent equations for x and y which we solve numerically in § 3. First, though, we consider two special cases.

(i) $\rho_3 = 0$

In this case we have a current flowing along a free surface. Equations (2.29) and (2.30) then simplify to

$$1 - 2x + \alpha'_{21}x^3(2-x) = 0 \tag{2.31}$$

and

$$H(1-\alpha'_{21}x^2) = 1-x.$$

Figure 6 shows graphically the solution to (2.31). For stable stratification we have $0 < \alpha'_2 < 1$. We see that for this problem the current thickness always remains close to one half.

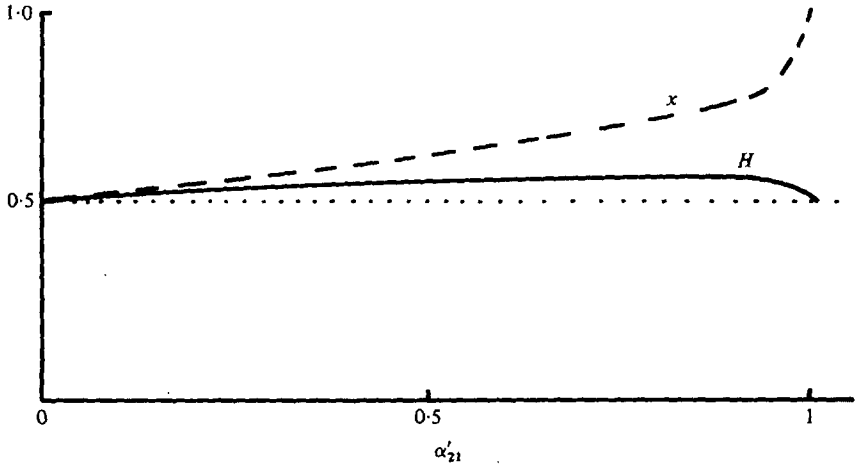

FIGURE 6. The energy-conserving solution for the intrusion when $\rho_3 = 0$.

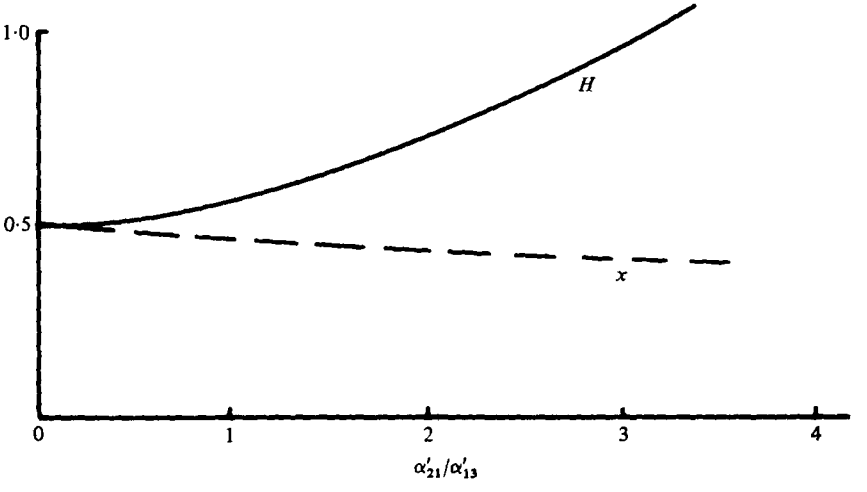

FIGURE 7. The energy-conserving solution for the intrusion when $Z \gg 1$.

(ii) $Z \gg 1$

From (2.30) with $Z \to \infty$, we obtain

$$H(1-\alpha'_{21}x^2) = (1-x)\left(1+\frac{\alpha'_{21}}{\alpha'_{13}}x^2\right). \tag{2.32}$$

Substituting into (2.29), we find that

$$1-2x+\alpha'_{21}x^3(2-x)-\frac{\alpha'_{21}}{\alpha'_{13}}x^4(1-\alpha'_{21}) = 0. \tag{2.33}$$

If the fluids are Boussinesq, so that $\alpha'_{21} \ll 1$, (2.33) reduces to

$$1-2x+\frac{\alpha'_{21}}{\alpha'_{13}}x^4 = 0. \tag{2.34}$$

The solution of (2.32) and (2.34) is shown in figure 7. There is always a unique solution for the depths x and H for given $\alpha'_{21}/\alpha'_{13}$. As $\rho_1 \to \rho_3$, $\alpha'_{21}/\alpha'_{13} \to \infty$ and $H \to \infty$. However, this solution breaks down for $H = O(Z)$, so there is no solution with the current height finite if $\alpha'_{21}/\alpha'_{13} \gg 1$. This is analogous to there being no energy-conserving solution for a boundary current entering homogeneous fluid. If $\alpha'_{21}/\alpha'_{13}$ is finite, an energy-conserving current can exist in the infinite-depth fluid.

3. The energy-conserving solutions

In this section we consider the results of solving the equations (2.8) and (2.9) for the boundary current and of solving (2.29) and (2.30) for the intrusion. For both boundary currents and intrusions it is found that, for a range of fluid depths and densities, the solution is not unique. This is a feature which also occurs for dissipative currents, for which it is necessary to use some extra condition in order to determine which solution will occur in practice. The condition suggested for dissipative currents is that the energy dissipation is a maximum for a given volume inflow rate. The only condition that can then be consistently applied to determine the solution for energy-conserving currents is that the volume inflow is a maximum. This is because, if there is an energy-conserving solution with a lower inflow rate, there is always found to be another solution at the same inflow rate, but with an energy loss. By the condition used for dissipative flows, that the solution with the largest energy loss occurs, the only energy-conserving solution which can be obtained is that with the maximum volume inflow rate.

3.1. *The boundary current*

The equations (2.8) and (2.9) were solved numerically using a double Newton–Raphson method. Two typical sets of results are shown in figure 8. The current height, H, and the lower layer depth, x, are plotted against α_{23}, for fixed values of α_{12} and Z. When $\alpha_{23} = 0$ there is only one solution with $H \neq 0$: $H = \frac{1}{2}Z$ and $x = \frac{1}{2}$. However, for $0 < \alpha_{23} < \alpha_c$, for some α_c dependent upon Z, there is no longer a unique solution. There are three non-trivial solutions. At α_c two of these solutions coalesce and for $\alpha > \alpha_c$ they no longer occur, leaving a unique solution as $\alpha_{23} \to \infty$. For larger values of α_{23} the solution becomes close to the free surface solution obtained in § 2.1. It can be shown numerically, using the analysis of appendix A, that each three-layer system corresponding to the solutions presented in figure 8 can support a hydraulic jump over the current. The stability to infinitesimal disturbances will be studied in § 5 when we can include dissipative currents.

Thus, for energy-conserving currents, there is frequently no unique solution. We have argued that the solution to occur in practice will be that with the largest volume inflow, $M = c_1 H$. From equations (2.1) and (2.3) we find $M^2 = c_1^2 H^2 = 2\alpha_{12} g H^3 x^2$. For the cases illustrated it has been calculated that the solution with the maximum value of M is always that with the largest value of H.

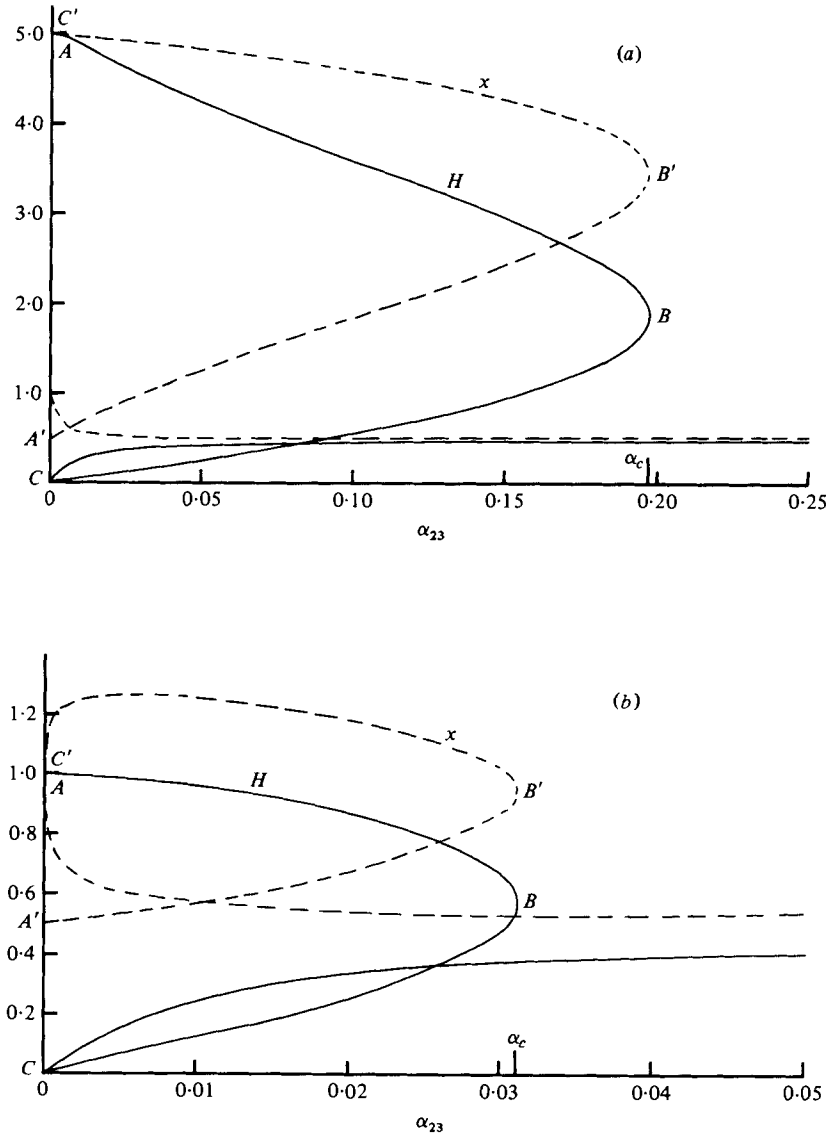

FIGURE 8. The energy-conserving solutions for the boundary current plotted against α_{23} for (*a*) $Z = 10$, $\alpha_{12} = 0{\cdot}01$ and (*b*) $Z = 2$, $\alpha_{12} = 0{\cdot}01$. The dashed line represents x and the solid line H. As H varies along the curve ABC, x varies along the curve $A'B'A$.

3.2. *The intrusion*

Equations (2.29) and (2.30) were solved for the intrusion. Two typical sets of results are shown in figure 9. In appendix B, we show that the solutions are such that not both

$$F_B^2 = \frac{c_2^2}{\alpha'_{21} g x} < 1 \quad \text{and} \quad F_T^2 = \frac{c_3^2}{\alpha'_{13} g y} < 1. \tag{3.1}$$

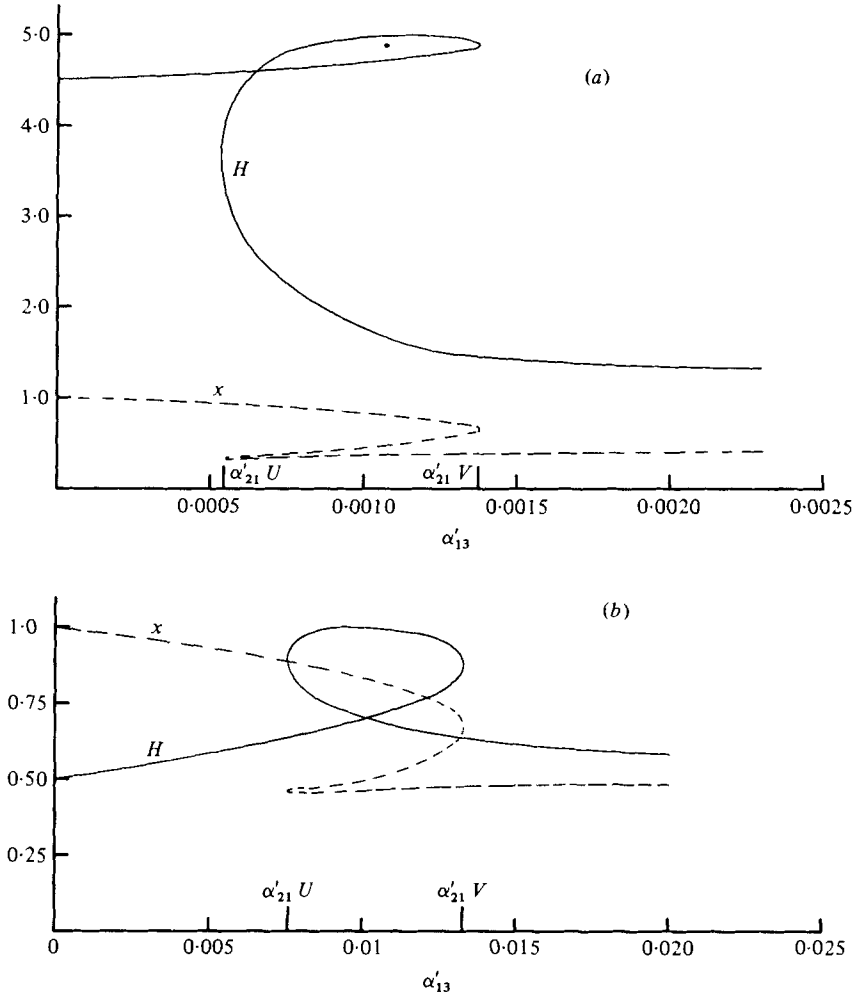

FIGURE 9. The energy-conserving solutions for the intrusion plotted against α'_{13} for (*a*) $Z = 10$, $\alpha'_{21} = 0{\cdot}01$ and (*b*) $Z = 2$, $\alpha'_{21} = 0{\cdot}01$. The dashed line represents x and the solid line H.

It is also shown that there will be three solutions for a range of $\alpha'_{21}/\alpha'_{13}$. For Boussinesq currents with $\alpha'_{21} \ll 1$ and $\alpha'_{13} \ll 1$ the range in which there are three solutions can be given explicitly by

$$U < \alpha'_{13}/\alpha'_{21} < V, \tag{3.2}$$

where

$$U = 27/(Z^{\frac{1}{2}}+3)^3(Z^{\frac{1}{2}}-1) \quad \text{and} \quad V = [3(Z-1)^{\frac{1}{2}}+Z^{\frac{1}{2}}]^3/\{27[(Z-1)^{\frac{1}{2}}+Z^{\frac{1}{2}}][Z-1]^2\}.$$

These positions are shown in figure 9. In figure 10, U and V are plotted as functions of Z.

For a symmetrical current, by which we mean one with $Z = 2$ and $\alpha'_{21} = \alpha'_{13}$, there are always three energy-conserving solutions, not just one solution near $x = \frac{1}{2}$, $y = \frac{1}{2}$ and $H = 1$. Again, however, the solution we expect to obtain is that which has the

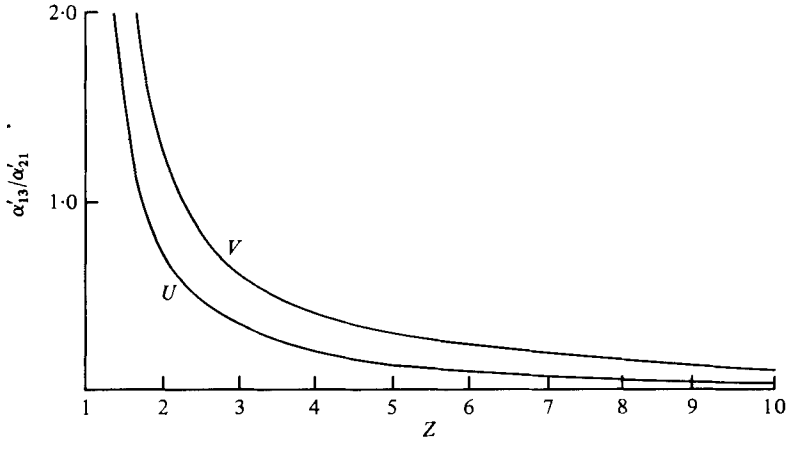

FIGURE 10. U and V plotted as functions of Z.

maximum value of M ($= c_1 H$). For the symmetrical current, this is the solution with x and y approximately one half and H approximately one.

4. Dissipative currents

We now consider currents that do not conserve energy. If the volume inflow, M, is specified, then unless the volume inflow happens to be exactly that required for the energy-conserving current, the current cannot conserve energy. A model of dissipation is used which allows a uniform head loss down streamlines. This is a simple model, but is sufficient to give a basic idea of the physics involved and is identical to that used by Benjamin (1968). We make frequent use of the Boussinesq approximation, which allows the effects of density differences to be neglected unless they are incorporated with gravity. This is equivalent to assuming each of the quantities α_{ij} and α'_{ij} to be small.

It is now found that a continuum of solutions is possible. The energy loss, E, is evaluated as a function of x and y, the downstream depths. If the volume inflow, $M(x, y)$, is given, then we can determine y as a function of x. But we still have a one-parameter family of apparently obtainable solutions. We obtain a unique solution by supposing that the solution with maximum energy loss occurs. It is envisaged that, if the system has an energy loss below the maximum, it will lose more energy until the energy loss reaches a maximum. Hence the solution which will occur is found by maximizing $E(x, y)$ subject to $M(x, y)$ being constant.

4.1. *The boundary current*

The system we consider is exactly as before, but now we suppose there is a uniform energy loss, D_1, in the ρ_2-fluid above the current, OD, and a uniform energy loss, D_2, in the ρ_3-fluid above OD.

We define head losses

$$\Delta_1 = D_1/\rho_2 c_1 g, \quad \Delta_2 = D_2/\rho_3 c_1 (Z-1) g.$$

Then the energy equations (2.3) and (2.5) are changed to include the energy dissipation, and become

$$c_2^2 = 2\alpha_{12} g(H - \Delta_1/\alpha_{12}) \tag{4.1}$$

and

$$p_2/\rho_3 = \alpha_{23} g(1-x) - \alpha_{13} gH + \tfrac{1}{2}c_3^2 - \tfrac{1}{2}c_1^2 + g\Delta_2. \tag{4.2}$$

The remaining equations (2.1)–(2.6) stay exactly as before, and we can manipulate the equations to obtain expressions for Δ_1 and Δ_2. Defining

$$P = \alpha_{12}(1+\alpha_{23})(2Z-H)H + \alpha_{23}[(Z-1)^2 - y^2],$$

$$Q = 2x\{(1+\alpha_{23})(2-x) + x(Z-1)[2(Z-1) - y + \alpha_{23}y]/y\},$$

$$R = Qy^2/x^2(Z-1)^2,$$

we find that

$$\Delta_1 = \alpha_{12}H - P/Q \tag{4.3}$$

and

$$\Delta_2 = \alpha_{12}(1+\alpha_{23})H + \alpha_{23}(H+x-1) - (P/R)[1 + \alpha_{23}y^2(Z-1)^{-2}]. \tag{4.4}$$

Thus, using (4.3) and (4.4) we can determine Δ_1 and Δ_2, given x and y. If $\Delta_1 = \Delta_2 = 0$ then we return to the energy-conserving currents of the previous section. We suppose there is no outside agency putting energy into the system and so only solutions with $E = D_1 + D_2 \geqslant 0$ are acceptable. One of D_1 or D_2 is, however, allowed to be negative, since energy can be transferred across the interface AB. So we now have a continuum of solutions for the current and layer depths.

As already suggested, the solution which will be attained is that which has the maximum (positive) value of E subject to M held constant. Using the method of Lagrange for finding extremals of functions subject to constraints, the above condition can be written as

$$\frac{\partial M}{\partial x}\frac{\partial E}{\partial y} = \frac{\partial M}{\partial y}\frac{\partial E}{\partial x} \tag{4.5}$$

with

$$M = \text{constant}, \tag{4.6}$$

provided that the solution found is a maximum, and not any other stationary value.

We now make the Boussinesq approximation, by assuming $\alpha_{12}, \alpha_{13} \ll 1$. Then substituting the known functions E and M into (4.5) and differentiating, we obtain

$$\begin{aligned}
&\frac{3c_1^2}{xyD}\left(\frac{1}{x^2} + \frac{(Z-1)^2}{y^2}\right)\{c_1^2[y^2 - x^2(Z-1)^2] + \alpha_{23}x^2y^3\} \\
&\quad + \frac{2}{D}(Z-x-y)\frac{c_1^2}{x^2y^2}\{c_1^2(Z-1)^2[y - x(Z-1)] - \alpha_{12}(x+y)[y^3 - x^3(Z-1)^3] - \alpha_{23}y\} \\
&\quad + \frac{2\alpha_{23}}{xyD}(Z-1)c_1^2[y^2(1-x) + x^2(Z-1)^3 - x^2y(Z-1)^2] \\
&\quad - \alpha_{12}x^2y^2(x+y)(Z-x-y) - \alpha_{23}x^2y^3(Z-1-y) \\
&\quad - \frac{2c_1^4}{x^3y^3}[y^3 - x^3(Z-1)^3] - 2\alpha_{23}(Z-1)c_1^2 = 0,
\end{aligned} \tag{4.7}$$

where

$$D = 2x(Z-1)^2 + (2-xZ)y \quad \text{and} \quad c_1^2 = 2x^2P/Q.$$

In general (4.6) and (4.7) must be solved numerically.

The only situation in which the solution is easily obtained analytically is when $\alpha_{23} = 0$, that is when the current is entering homogeneous fluid. The solution of (4.7) is then $y = x(Z-1)$. Then

$$\Delta_1 = \Delta_2 = \alpha Z(1-x)^2(2x-1)/2x(2-x) \tag{4.8}$$

and

$$E = \rho_3 g c_1 Z \Delta_1. \tag{4.9}$$

These agree with Benjamin (1968). Now $E \geqslant 0$ only for $\frac{1}{2} \leqslant x \leqslant 1$, so only solutions in this range are possible.

4.2. *The intrusion*

Energy losses are incorporated into intrusions in a similar way to that used for boundary currents. We assume there is an energy loss D_1 in the region beneath OC and an energy loss D_2 in the region above OB, and that no energy is lost upstream of O. We define Δ_1 and Δ_2 by

$$\Delta_1 = D_1/\rho_2 c_1 g, \quad \text{and} \quad \Delta_2 = D_2/\rho_3 c_1 (Z-1) g.$$

The point O will remain a stagnation point and the only equations that change are (2.26) and (2.27), which become

$$c_2^2(1-\alpha'_{21}x^2) = 2\alpha'_{21} g(1-x-\Delta_1/\alpha'_{21}) \tag{4.10}$$

and

$$c_3^2[1+\alpha'_{13}y^2/(Z-1)^2] = 2\alpha'_{13} g[Z-1-y-\Delta_2/\alpha'_{13}]. \tag{4.11}$$

We now define

$$P = [\alpha'_{21}(1+\alpha'_{13})(1-x^2)/(1-\alpha'_{21}) + \alpha'_{13}((Z-1)^2-y^2)][1-\alpha'_{21}x^2],$$

$$Q = 2x\{(1+\alpha'_{13})(2-x-\alpha'_{21}x)/(1-\alpha'_{21}) + (x/y)(Z-1)[2(Z-1)-y+\alpha'_{13}y]\}$$

and

$$R = Qy^2/x^2(Z-1)^2.$$

Then

$$\Delta_1 = \alpha'_{21}(1-x) - P/Q, \tag{4.12}$$

$$\Delta_2 = \alpha'_{13}(Z-1-y) - (P/R)\{1+[\alpha'_{13}y^2/(Z-1)^2]\}/(1-\alpha'_{21}x^2), \tag{4.13}$$

$$c_1^2 = 2x^2 Pg/(1-\alpha'_{21}x^2)Q \tag{4.14}$$

and

$$E = \rho_3 c_1 g\{(1+\alpha'_{13})\Delta_1/(1-\alpha'_{21}) + (Z-1)\Delta_2\}. \tag{4.15}$$

For the intrusion we allow only solutions with $\Delta_1 > 0$ and $\Delta_2 > 0$, since there can be no transfer of energy through the current. We again impose the condition that E is a maximum subject to M constant. If $\alpha'_{21}, \alpha'_{13} \ll 1$ this condition can be written as

$$\begin{aligned}
&2[c_1^2(Z-1)^2-\alpha'_{13}y^3]\frac{x}{yD}\left[(Z-1-y)[\alpha'_{13}(Z-1)-\alpha'_{21}]+(Z-x-y)\frac{c_1^2}{gx^3}\right.\\
&\left.-\frac{3c_1^2}{2g}\left(\frac{1}{x^2}+\frac{(Z-1)^3}{y^2}\right)\right]+\frac{2c_1^2}{gy^3}(Z-1)[c_1^2(Z-1)^2-\alpha'_{13}y^3]\\
&+\frac{2y}{xD}(c_1^2-\alpha'_{21}x^3)\left[(1-x)(\alpha'_{13}(Z-1)-\alpha'_{21})\right.\\
&\left.-(Z-x-y)\frac{c_1^2}{gy^3}(Z-1)^3+\frac{3c_1^2}{2g}\left(\frac{1}{x^2}+\frac{(Z-1)^2}{y^2}\right)\right]\\
&-\frac{2c_1^2}{gx^3}(c_1^2-\alpha'_{21}x^3)=0, \qquad (4.16)
\end{aligned}$$

where

$$D = 2x(Z-1)^2+(2-xZ)y \quad \text{and} \quad c_1^2 = 2x^2P/Q.$$

In general, (4.16) must be solved numerically. However, if $\alpha'_{21} = \alpha'_{13}(Z-1)$ then the solution of (4.16) can be shown to be $y = x(Z-1)$. We have already called this the symmetrical current (§ 3), since it sits symmetrically between the top and bottom. For the symmetrical current

$$\Delta_1 = \Delta_2 = \tfrac{1}{2}\alpha'_{13}(1-x)^2(2x-1)(Z-1)/x(2-x) \qquad (4.17)$$

and

$$E = Z\Delta_1\rho_3 c_1 g.$$

From the above equation it can be seen that the energy-conserving solution has $x = \frac{1}{2}, y = \frac{1}{2}(Z-1), H = \frac{1}{2}Z$. This is the solution obtained in § 3 for the symmetrical current.

This symmetrical current has some similarities with the boundary current entering homogeneous fluid, as there is almost a plane of symmetry through the upstream interface. However, it is not precisely a plane of symmetry since the point O must be raised above the upstream level in order to satisfy the condition of continuity of pressure. The most fundamental difference between the symmetrical current and the bottom current occurs in the stability of the system, which we discuss in the next section.

5. Stability

We examine the stability of the system as shown in figure 11 to infinitesimal wave-like disturbances. We have introduced surface tension at each interface; otherwise short waves would always be unstable. Although there is always surface tension between two immiscible fluids, provided it is weak enough the addition of surface tension will affect only the deformed shape of the current head and the stability of the current downstream. The surfaces at $z = H_1$ and $z = H_1+H_2$ are displaced to $z = H_1+\eta(x,t)$ and $z = H_1+H_2+h(x,t)$. We suppose that the displacements h and η

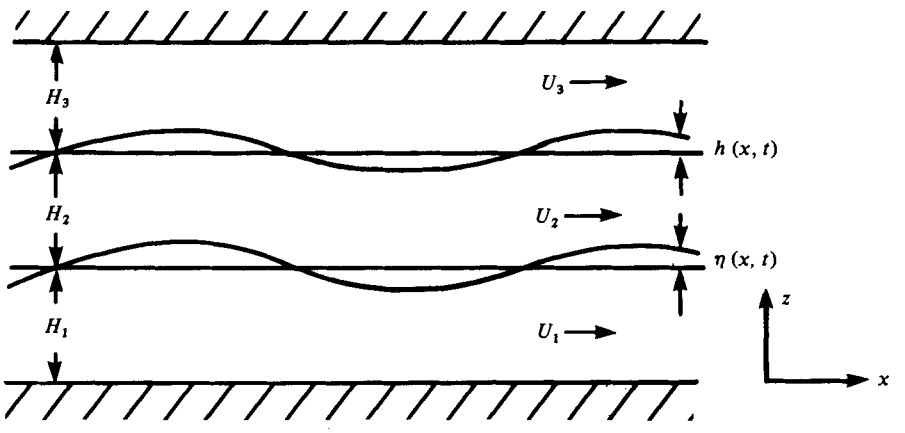

FIGURE 11. The three-layer system. There is a surface tension T_{23} between the ρ_2' and ρ_3' fluids and a surface tension T_{12} between ρ_1' and ρ_2' fluids. For the boundary current take $U_1 = 0$, $U_2 = c_2$, $U_3 = c_3$, $H_1 = H$, $H_2 = x$, $H_3 = y$ and $\rho_i' = \rho_i$ for $i = 1, 2, 3$. For the intrusion take $U_1 = c_2$, $U_2 = 0$, $U_3 = c_3$, $H_1 = x$, $H_2 = H$, $H_3 = x$ and $\rho_1' = \rho_2$, $\rho_2' = \rho_1$, and $\rho_3' = \rho_3$.

are infinitesimal and look to see whether they grow or decay with time. If we look for solutions with

$$\eta = \eta_0 \exp[ik(x-ct)]$$

and

$$h = h_0 \exp[ik(x-ct)],$$

then using standard methods we obtain the dispersion relation

$$\begin{aligned}[\rho_1'(c-U_1)^2 k \coth kH_1 + \rho_2'(c-U_2)^2 k \coth kH_2 - (\rho_1'-\rho_2')g \\ - T_{12}k^2][\rho_3'(c-U_3)^2 k \coth kH_3 + \rho_2'(c-U_2)^2 k \coth kH_2 \\ - (\rho_2'-\rho_3')g - T_{23}k^2] - [\rho_2'^2(c-U_2)^4 k^2/\sinh^2 kH_2] = 0, \end{aligned} \tag{5.1}$$

where T_{ij} is the surface tension between the ρ_i'- and the ρ_j'-fluids.

Equation (5.1) is a quartic in c. If it has four real roots for $c = c(k)$ then the system will be stable. If it has a pair of complex-conjugate roots then there will be a solution which grows exponentially with time and the system will be unstable.

Given a polynomial such as (5.1) it is possible to find the number of real and complex roots it possesses by setting up a Sturm sequence of polynomials (see Burnside & Panton 1960). When approached numerically this is a very useful method, although it is hard to use analytically as the expressions involved become rather complicated. Alternatively, if we write (5.1) as

$$a'c^4 + 4b'c^3 + 6c'c^2 + 4d'c + e' = 0 \tag{5.2}$$

and define

$$S = a'e' - 4b'd' + 3c'^2$$

and

$$T = a'c'e' + 2b'c'd' - a'd'^2 - e'b'^2 - c'^3,$$

then (5.2) has four real roots if and only if (Salmon 1866)

$$S^3 - 27T^2 > 0, \quad b'^2 - a'c' > 0, \quad 3a'T + 2(b'^2 - a'c')S > 0. \tag{5.3}$$

We shall consider the stability of the current downstream from the stagnation point of a symmetrical intrusion, with $Z = 2$ and $\alpha'_{21} = \alpha'_{13} \ll 1$. From § 4 we know that any such current will have $x = y$. By using the conditions (5.3) it is possible to show analytically that long waves are always stable for any intrusion with a non-negative energy loss. It is known that short waves will be stabilized by surface tension. So we expect to find a range of wavenumbers (k_1, k_2) for which the system will be unstable. If the surface tension is sufficiently large, this range will be empty, and the flow will be stable everywhere.

For a current with $x = y = 0{\cdot}7$ and $T_{12} = T_{23}$, using the Sturm polynomials, we find the current downstream is stable for all wave-numbers if

$$T_{12}/\rho_1 g d_1^2 \geqslant 5 \times 10^{-4}$$

and unstable for

$$\pi \leqslant k \leqslant 9\pi/2 \quad \text{if} \quad T_{12}/\rho_1 g d_1^2 = 2{\cdot}5 \times 10^{-4}.$$

For simplicity we shall consider only the case of $\rho_2 = \rho_3$ for the boundary current and suppose there is no surface tension between the ρ_2- and ρ_3-fluids. The dispersion relation for this system is

$$\rho_1 kc^2 \coth kH + \rho_2 (c - c_2)^2 k \coth k(x+y) = (\rho_1 - \rho_2) g + T_{12} k^2.$$

This is a quadratic equation and the condition for it to have two real roots is easily found to be

$$k^{-1}\{[\tanh kH/(1+\alpha_{12})] + \tanh k(x+y)\}\{1 + [T_{12} k^2/\alpha_{12}\rho_2 g Z^2]\} > c_2^2/\alpha_{12} g.$$

If $x + y = 0{\cdot}7Z$ then the current is stable for $T_{12}/\rho_1 g Z^2 = 2{\cdot}5 \times 10^{-4}$. The symmetrical intrusion is unstable at this surface tension.

We can see from the two numerical examples cited that the stability of the intrusions is both physically and numerically very different to the stability of the boundary current entering a homogeneous fluid. The stability of the system is very important, since if the system is unstable Kelvin–Helmholtz billows will form on the interface and lead to a large amount of mixing.

Unfortunately we know of no gravity current experiments which have used immiscible fluids, so it is not possible to make a direct comparison of these results with experiments. Although experiments which study boundary currents in miscible fluids have always had Kelvin–Helmholtz billows downstream, we predict that experiments using immiscible fluids with sufficiently high surface tension would result in stable boundary currents.

6. Downstream waves

In § 4 we considered dissipative currents. If the volume inflow into the current is higher than the critical value the flow downstream will be supercritical and, since stationary waves cannot form on a supercritical stream, the energy loss, which must still occur, will have to be by turbulence and small-scale viscous dissipation. However, if the volume inflow is sufficiently low, the flow will be subcritical downstream and this will allow the necessary energy loss to occur by the formation of a stationary wave train behind the current head. A stationary wave train is one for which the phase

speed, c, of the waves is zero relative to the motion of the current. There are four wave modes in any three-layer system, so there will be two stationary wave modes, as we show below.

If we look for stationary waves of infinitesimal amplitude then we can use the dispersion relation (5.1) to calculate their wavelengths, by setting $c = 0$. For the intrusion, where $c = U_2 = 0$, we find

$$(F_B^2 kx - \tanh kx)(F_T^2 ky - \tanh ky) = 0, \tag{6.1}$$

where

$$F_B^2 = c_2^2/\alpha'_{21} gx \quad \text{and} \quad F_T^2 = c_3^2/\alpha'_{13} gy.$$

Provided the flow is subcritical, this gives two solutions for k, given by the solutions of

$$F_B^2 kx = \tanh kx \quad \text{and} \quad F_T^2 ky = \tanh ky.$$

The first of these solutions has the amplitude on the upper interface, h_0, equal to zero and a non-zero amplitude on the lower interface, and the second solution has the amplitude on the lower interface, η_0, equal to zero and a non-zero amplitude on the upper interface. Thus the system of stationary waves will have one wavelength on the lower interface and a different wavelength on the upper.

The amplitudes of the waves can be calculated by relating the energy losses D_1 and D_2 to the energy flux radiated away by the waves, namely the wave energy times the group velocity:

$$D_1 = \tfrac{1}{4} c_2 \rho_2 \alpha'_{21} g \eta_0^2 [1 - 2kx/\sinh 2kx] \tag{6.2a}$$

and

$$D_2 = \tfrac{1}{4} c_3 \rho_3 \alpha'_{13} g h_0^2 [1 - 2ky/\sinh 2ky]. \tag{6.2b}$$

When typical laboratory values are inserted into these equations, it is generally found that the amplitudes h_0 and η_0 are not small compared with the wavelength. If D_1 and D_2 are small, this infinitesimal theory may be reasonable, but generally the amplitudes are too large and we need to consider nonlinear waves.

The nonlinear problem is solved by setting it up as a perturbation expansion in the wave amplitude, a. We have worked only as far as third order in a. As shown in appendix C, the waves on each interface are equivalent to surface waves moving under reduced gravity. The high-order perturbation theory results of Cokelet (1977) for surface waves on a finite-depth layer could be used to calculate the amplitudes and wavelengths. However, Cokelet's results for only ten separate depths do not cover the range sufficiently closely to obtain accurate estimates for the amplitudes. Comparisons of the wavelengths calculated from our third-order theory and Cokelet's higher-order results indicate that the third-order theory may underestimate the wavelength by up to 20 %.

The wavelength of the wave on the lower interface is now given by

$$k = k_0 + a^2 k_1, \tag{6.3}$$

where k_0 is the root of

$$F_B^2 kx = \tanh kx$$

and

$$k_1 = \tfrac{1}{8} k_0^3 (9 \coth^4 k_0 x - 10 \coth^2 k_0 x + 9)/[1 - 2k_0 x/\sinh 2k_0 x].$$

$x\,(=y)$ layer depths	$\Delta_1/\alpha'_{21} = \Delta_2/\alpha'_{13}$ energy losses	$c_2/\alpha'^{\frac{1}{2}}_{21} = c_3/\alpha'^{\frac{1}{2}}_{13}$ layer velocities	$F_B^2\,(=F_T^2)$ Froude numbers	Wavelength to first order	Wavelength to third order	a, wave amplitude
0·95	$1{\cdot}13\times10^{-3}$	0·313	0·103	0·614	0·417	0·065
0·9	$4{\cdot}04\times10^{-3}$	0·438	0·213	1·21	0·839	0·121
0·85	$8{\cdot}06\times10^{-3}$	0·533	0·334	1·79	1·28	0·163
0·8	$1{\cdot}25\times10^{-2}$	0·612	0·469	2·43	1·75	0·196
0·75	$1{\cdot}67\times10^{-2}$	0·683	0·622	3·29	2·24	0·220
0·7	$1{\cdot}98\times10^{-2}$	0·749	0·801	4·96	2·71	0·211
0·68	$2{\cdot}06\times10^{-2}$	0·774	0·881	6·62	2·73	0·176
0·66	$2{\cdot}09\times10^{-2}$	0·799	0·967	12·90	2·04	0·095

TABLE 1. Wavelengths for the symmetrical current with $Z = 2$ and $\alpha'_{21}/\alpha'_{13} = 1$, $\alpha'_{21}, \alpha'_{13} \ll 1$.

In order to find the wavelength, we need to know the amplitude of the waves. This we calculated from the energy to obtain

$$D_1 = c_2\rho_2\alpha'_{21}a^2g\left[\frac{1}{4}\left(1-\frac{2k_0x}{\sinh 2k^0x}\right)+a^2k_0\left(\tfrac{9}{64}ch^6-\tfrac{3}{8}ch^4+\tfrac{21}{64}ch^2-\tfrac{9}{32}\right.\right.$$
$$-\frac{k_0x}{\sinh 2k_0x}\frac{1}{(1-2k_0x/\sinh 2k_0x)}\left(\tfrac{21}{32}ch^4-\tfrac{19}{32}ch^4+\tfrac{9}{16}\right.$$
$$\left.\left.\left.-k_0x(\tfrac{21}{16}ch^5-\tfrac{5}{4}ch^3+\tfrac{37}{32}ch-\tfrac{9}{16}th)\right)\right)\right], \qquad (6.4)$$

where $ch = \coth k_0x$ and $th = \tanh k_0x$. The equations for the wave on the upper interface are similar.

For the symmetrical intrusion the wavelengths obtained for different values of the volume inflow are shown in table 1. We have taken $Z = 2$ and $\alpha'_{21}/\alpha'_{13} = 1$ with $\alpha'_{21}, \alpha'_{13} \ll 1$. For this case the amplitudes and wavelengths for the waves on the upper and lower interfaces are the same. If $\alpha'_{21} < \alpha'_{13}$ and $Z = 2$, then the wavelength is longer on the upper interface than on the lower. If $\alpha'_{21} > \alpha'_{13}$ and $Z = 2$, then the wavelength is shorter on the upper interface. Using equations (6.3) and (6.4) it is possible to calculate the amplitudes and wavelengths of the stationary waves behind the head quite easily for any intrusion.

We show in figures 12, 13 and 14 examples of intrusions. They were obtained by John E. Simpson of DAMTP by setting up a two-layer system of salt water in a tank with salt water of intermediate density behind a lock at one end. The lock was then raised to form the current. There are several differences between his experimental set-up and this theory. The main difference is that the volume inflow to the current is not specified and it will decrease as the lock empties. Also reflexions from the back wall can catch up with the current and cause shocks at the front, although by making the lock long these reflexions take a long time to reach the front, making it possible to carry out the experiments without the problem of reflexion arising.

For figure 12 the current is almost symmetrical with $Z = 2$, $\alpha'_{21} = 1{\cdot}48\times10^{-2}$, $\alpha'_{13} = 1{\cdot}52\times10^{-2}$ and $d_1 = 5$ cm. Since the volume inflow to the current is not known, we cannot use the theory to calculate the downstream fluid depths, although it does predict that the upper depth, y, should be very nearly equal to the lower depth, x.

From figure 12 we can measure x and y and find that $x \approx y \approx 0{\cdot}7d_1$. Using equation (4.14), we predict that the velocity of the current should be 4·49 cm s^{-1}. The wavelengths, as given by (6.3) and (6.4), are 13·0 cm on the lower interface and 14·2 cm on the upper interface. The wave amplitude is predicted to be 1·1 cm on each interface. The velocity, c_1, for this experiment was measured as 3·9 cm s^{-1}, which is 12 % smaller than the value predicted theoretically. Waves can be seen on each interface. The wavelength on the lower interface is about 12·5 cm on the lower interface and 14·0 cm on the upper interface. So we see that the theory has predicted the wavelength rather accurately, although the theoretical calculations were only to third order. The reasons that the wavelengths are different on the upper and lower interfaces are that, first, the current is not quite symmetrical and, second, it is not quite Boussinesq. The amplitude of the waves cannot be easily measured because of the mixing between the fluids, although it can be estimated as 1·2 cm, which is consistent with the predicted value. In § 2, we predicted that the angles at the front of the current should be 120° and that the current should be slightly 'sunk'. The angles at the front of the current cannot really be determined from the experiments, as the interfaces are not sharp as assumed. However, it does seem possible that the 120° angles could fit, and the orientation is almost horizontal with the current 'sunk' slightly.

For figure 13 $Z = 1{\cdot}5$, $\alpha'_{21} = 4{\cdot}99 \times 10^{-3}$, $\alpha'_{13} = 1{\cdot}01 \times 10^{-2}$ and $d_1 = 6{\cdot}7$ cm. The depths x and y must be measured as before and $x \approx 0{\cdot}76d_1$ and $y \approx 0{\cdot}39d_1$. The current velocity predicted by (4.14) is then 2·85 cm s^{-1}. The wavelengths given by (6.3) and (6.4) are 5·5 cm on the upper interface and 13·7 cm on the lower interface. The amplitudes are predicted as 1·5 cm on the lower interface and 0·6 cm on the upper interface. The current velocity was measured as 3·85 cm s^{-1}, which is 30 % larger than the theoretical value. The upper wavelength was measured as about 5 cm and the lower as 14 cm. The lower interface shows signs of mixing and this is probably due to shear instability, as the waves on the lower interface are much longer and less steep than those on the upper interface, which are not breaking. At the front stagnation point, the current is 'sunk' and the system of 120° angles is rotated so that $\beta < 0$ because the current is heavier than the average density.

For figure 14 $Z = 3$, $\alpha'_{21} = 1{\cdot}97 \times 10^{-2}$, $\alpha'_{13} = 1{\cdot}01 \times 10^{-2}$ and $d_1 = 2{\cdot}3$ cm. The depths x and y are approximately $0{\cdot}67d_1$ and $1{\cdot}34d_1$. The flow over the intrusion is almost supercritical. The current velocity predicted by (4.14) is 3·65 cm s^{-1}. The wavelengths given by (6.3) and (6.4) are 6·1 cm on the lower interface and 24·1 cm on the upper interface. The amplitudes of these waves are predicted to be 0·3 cm and 0·5 cm. The current velocity was measured to be 3·75 cm s^{-1}, which is 5 % larger than the theoretical value. On the upper interface no wave can be seen and the interface shows signs of mixing. The predicted wavelength for this interface is, however, so long that the section of current shown is shorter than one wavelength and this may be why no wave can be seen. On the lower interface the beginnings of a wave can be seen about 6·2 cm from the front. This distance is close to the theoretically predicted wavelength. At the front the current is raised with respect to the horizontal upstream layer so that the angle is positive, as predicted.

Bearing in mind the differences between these lock exchange experiments and the theory under consideration, the comparison is good and it seems that the ideas introduced here are quantitatively correct for the experiments.

7. Conclusions

In this paper we have presented a theoretical study of gravity currents in a two-layer fluid. We have shown that energy-conserving gravity currents can exist in an infinitely deep two-layered fluid, in contrast to Benjamin's result that they cannot exist in homogeneous fluid of infinite depth. Unless the volume inflow rate to the current takes a certain fixed value, energy cannot be conserved between upstream and downstream sections. We find that the current depth is not always uniquely determined by the equations of motion and to obtain a unique solution we propose the condition that the energy dissipation by the current is a maximum for a fixed inflow rate. At the front of any intrusion there is a stagnation point where the streamlines meet at 120°. The system of 120° angles is rotated clockwise or anticlockwise (for a current propagating to the left) depending on whether the current is heavier or lighter than the average of the densities upstream. We have examined the consequences of allowing the energy which is lost by most currents to form a stationary wave train behind the current and calculated the amplitudes and wavelengths such waves would have. The theory was shown to agree well with the experiments.

We wish to thank John E. Simpson for allowing us to use the photographs of his laboratory experiments and Steve Thorpe for drawing our attention to his paper on two-layer fluids. The work was supported by grants from the Ministry of Defence (Procurement Executive), the Natural Environmental Research Council and from the National Science Foundation under grants ENG 75-02985 and ENG 77-27398.

Appendix A. Supercritical and subcritical flows

Following Benjamin (1966), we define a flow to be critical when it can support infinitesimal stationary long waves. Ahead of the gravity current, in the two-layer system, the velocity of long waves on the interface is (Lamb 1932, p. 371)

$$c^2 = (\rho_2 - \rho_3)(Z-1)gd_1/[\rho_2(Z-1)+\rho_3] \tag{A 1}$$

and the flow is supercritical if $c_1^2 > c^2$ and subcritical if $c_1^2 < c^2$. If the flow is supercritical upstream, no wave-motion can propagate ahead of the current. If the flow is subcritical upstream, the influence of the current may propagate ahead of it on the initiation of the flow; however, this is not relevant to the consideration of a steady current of the type considered in this paper, as explained in the introduction. Both boundary currents and intrusions can be either supercritical or subcritical depending on the values of the parameters.

Downstream of the gravity current head the flow is in three layers. The dispersion relation for long waves in a three-layer system is obtained by letting $k \to 0$ in (5.1), from which it is found that the phase speed, c, satisfies the quartic equation

$$\left[\frac{\rho_1'}{H_1}(c-U_1)^2+\frac{\rho_2'}{H_2}(c-U_2)^2-(\rho_1'-\rho_2')g\right]\left[\frac{\rho_3'}{H_3}(c-U_2)^2+\frac{\rho_2'}{H_2}(c-U_2)^2-(\rho_2'-\rho_3')g\right] - \frac{\rho_2'^2}{H_2^2}(c-U_2)^4 = 0, \tag{A 2}$$

where the quantities involved are as defined in § 5 and figure 11. Benjamin's (1966) discussion of critical flow can be extended to define a three-layer system as supercritical if and only if all long wave modes propagate downstream with respect to the gravity current.

To determine whether or not a system is supercritical it is necessary to find the condition that (A 2) has four long-wave solutions which propagate downstream (i.e. have $c > 0$). Restricting the investigation to stable systems, we assume that (A 2) has four real roots for c. The conditions for the stability of the waves are discussed in § 5. We write (A 2) as

$$Lc^4 + Kc^3 + Jc^2 + Hc + G = 0. \tag{A 3}$$

With U_1, U_2 and U_3 positive, it is easily found that $L > 0$, and $K < 0$. It can then be shown, by Descartes' rule of signs, that (A 3) will have four positive roots and the system will be supercritical only if

$$J > 0, \quad H < 0, \quad G > 0. \tag{A 4}$$

For the boundary current, we calculate from (A 2) that

$$G = -\left[\frac{\rho_3 c_3^2}{y} - (\rho_2 - \rho_3)g\right](\rho_1 - \rho_2)g + \frac{\rho_2 c_2^2}{x}\left[\frac{\rho_3 c_3^2}{y} - (\rho_1 - \rho_2)g\right],$$

$$H = -2\left(\frac{\rho_3 c_3}{y} + \frac{\rho_2 c_2}{x}\right)\left[\frac{\rho_2 c_2^2}{x} - (\rho_1 - \rho_2)g\right] + \frac{4\rho_2^2 c_2^2}{x^2} - 2\frac{\rho_2 c_2}{x}\left[\frac{\rho_3 c_3^2}{y} + \frac{\rho_2 c_2^2}{x} - (\rho_2 - \rho_3)g\right],$$

and

$$J = \left(\frac{\rho_2}{x} + \frac{\rho_3}{y}\right)\left[\frac{\rho_2 c_2^2}{x} - (\rho_1 - \rho_2)g\right] + \left(\frac{\rho_1}{H} + \frac{\rho_2}{x}\right)\left[\frac{\rho_3 c_3^2}{y} + \frac{\rho_2 c_2^2}{x} - (\rho_2 - \rho_3)g\right]$$
$$+ 4\left(\frac{\rho_3 c_3}{y} + \frac{\rho_2 c_2}{x}\right)\frac{\rho_2 c_2}{x} - \frac{6\rho_2^2 c_2^2}{x^2}.$$

For the intrusion we calculate that

$$G = \left[\frac{\rho_3 c_3^2}{y} - (\rho_2 - \rho_3)g\right]\left[\frac{\rho_2 c_2^2}{x} - (\rho_2 - \rho_1)g\right],$$

$$H = -2\frac{\rho_3 c_3}{y}\left[\frac{\rho_2 c_2^2}{x} - (\rho_2 - \rho_1)g\right] - 2\frac{\rho_2 c_2}{x}\left[\frac{\rho_3 c_3^2}{y} - (\rho_1 - \rho_3)g\right],$$

and

$$J = \left(\frac{\rho_3}{y} + \frac{\rho_1}{H}\right)\left[\frac{\rho_2 c_2^2}{x} - (\rho_2 - \rho_1)g\right] + \left(\frac{\rho_2}{x} + \frac{\rho_1}{H}\right)\left[\frac{\rho_3 c_3^2}{y} - (\rho_1 - \rho_3)g\right] + 4\rho_3 c_3 \rho_2 c_2 / xy.$$

We now define Froude numbers

$$F_B^2 = \rho_2 c_2^2/(\rho_2 - \rho_1)gx = c_2^2/\alpha'_{21}gx$$

and

$$F_T^2 = \rho_3 c_3^2/(\rho_1 - \rho_3)gy = c_3^2/\alpha'_{13}gy.$$

Then one sees that $G > 0$ if and only if $F_B^2 > 1$ and $F_T^2 > 1$ or if $F_B^2 < 1$ and $F_T^2 < 1$. Now if $F_B^2 > 1$ and $F_T^2 > 1$, then $H < 0$ and $J > 0$, and so this represents a

supercritical flow. If $F_B^2 < 1$ and $F_T^2 < 1$, then $H > 0$, so this represents a subcritical flow. Hence the flow around an intrusion is supercritical if

$$F_B^2 > 1 \quad \text{and} \quad F_T^2 > 1 \tag{A 5}$$

and it is subcritical otherwise.

Appendix B. Energy-conserving solutions for intrusions

In this appendix we prove that all solutions of the energy-conserving equations for the intrusion (2.29) and (2.30) have at least one of F_T^2 and F_B^2 greater than unity and the flow can thus support a hydraulic jump. Using the expressions (2.26) and (2.27) for the velocities we obtain

$$F_B^2 = 2(1-x)/x(1-\alpha'_{21}x^2) \quad \text{and} \quad F_T^2 = 2(Z-1-y)/y[1+\alpha'_{13}y^2(Z-1)^{-2}]. \tag{B 1}$$

Only solutions with $x \leqslant 1$ and $y \leqslant Z-1$ will be possible since otherwise the velocities, as given by (2.26) and (2.27), become imaginary.

The governing equations for the intrusion (2.30) and (2.29) can be written as

$$E \equiv \frac{\alpha'_{21}(1-x)x^2}{1-\alpha'_{21}x^2} - \frac{\alpha'_{13}(Z-1-y)y^2}{(Z-1)^2+\alpha'_{13}y^2} = 0 \tag{B 2}$$

and

$$f \equiv \frac{\alpha'_{21}(1+\alpha'_{13})(1-x)^2(2x-1-\alpha'_{21}x^2)}{(1-\alpha'_{21})(1-\alpha'_{21}x^2)} + \frac{\alpha'_{13}(Z-1-y)^2[2y(Z-1)-(Z-1)^2+\alpha'_{13}y^2]}{(Z-1)^2+\alpha'_{23}y^2}. \tag{B 3}$$

Considering (B 3) as an equation for x, given y, one finds $\partial E/\partial x = 0$ when $x = 0$, corresponding to a minimum for E, and also when $2-3x+\alpha'_{21}x^3 = 0$, which occurs when $F_B^2 = 1$, corresponding to a maximum for E. In figure 15, E is plotted as a function of x for a particular value of y. It reaches a maximum value when $F_B^2 = 1$ and can be shown to be negative at $x = 0$ and $x = 1$ for all values of y. Solutions for the lower values of x have $F_B^2 > 1$. Hence, given a value for y, there will be a solution for x only if $E > 0$ where $F_B^2 = 1$ and, if this is the case, there will be two solutions for x, one with $F_B^2 > 1$ and the other with $F_B^2 < 1$.

We now consider (B 3) as an equation for y, given x. It can be shown that f has a minimum value when $y = Z-1$ and a maximum value at a value of y such that $F_T^2 = 1$. At $y = Z-1$, f is positive or negative according to whether $2x-1-\alpha'_{21}x^2$ is positive or negative. At the value of y for which $F_T^2 = 1$, f is positive if $2x-1-\alpha'_{21}x^2$ is positive. So, as shown in figure 16, we have two situations which depend on the sign of $2x-1-\alpha'_{21}x^2$.

Suppose both F_T^2 and F_B^2 are less than unity. From (B 1), $F_B^2 < 1$ if and only if $3x-2-\alpha'_{21}x^3 > 0$, but, since $2x-1-\alpha'_{21}x^2 > 3x-2-\alpha'_{21}x^3$ for all x, if $F_B^2 < 1$ then $2x-1-\alpha'_{21}x^2 > 0$ and the solution for y will be as shown in figure 16(*b*) with $F_T^2 > 1$. Hence there can be no solution to (B 2) and (B 3) which has $F_B^2 < 1$ and $F_T^2 < 1$.

We now determine the range of $\alpha'_{21}/\alpha'_{13}$ for which there can be three solutions for x and y. In order to obtain a result analytically we assume the fluids to be Boussinesq so that $\alpha'_{21}, \alpha'_{13} \ll 1$. First we look to see when we will get a double root for y. From

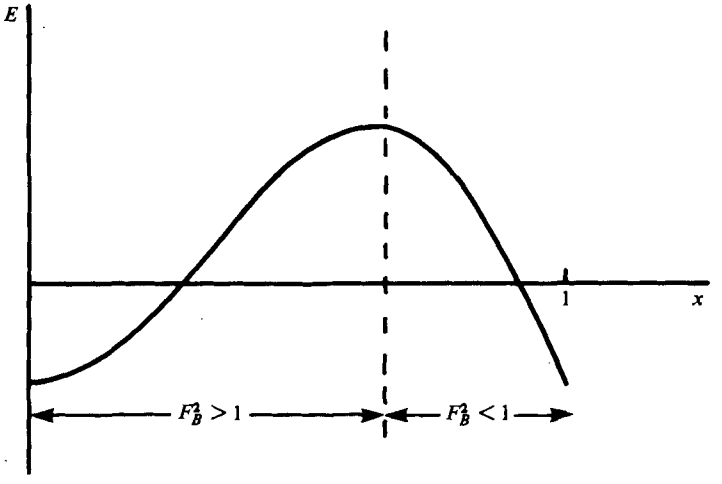

FIGURE 15. A plot of E as a function of x.

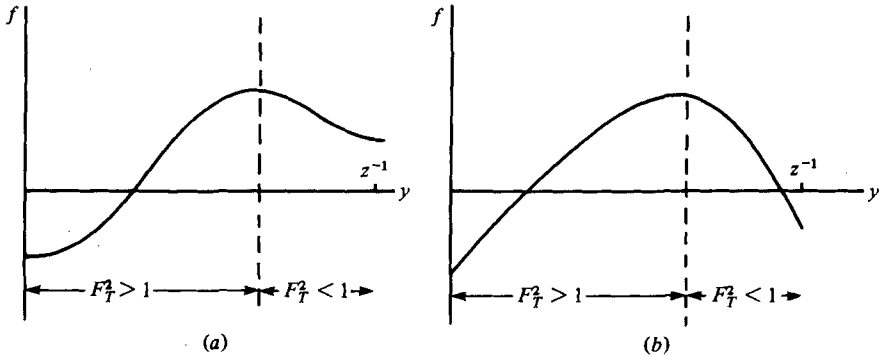

FIGURE 16. A plot of f as a function of y. In (*a*) $2x-1-\alpha'_{21}x^2 < 0$. The value of f at $F_T^2 = 1$ is always positive. In (*b*) $2x-1-\alpha'_{21}x^2 > 0$. The value of f at $F_T^2 = 1$ can be positive or negative.

figure 16(*b*) we see this occurs at the value of y for which $F_T^2 = 1$ if the value of f at that point is zero. Now if $F_T^2 = 1$, then $y = \frac{2}{3}(Z-1)$ as the fluids are Boussinesq. Hence

$$\tfrac{1}{27}\alpha'_{13}(Z-1)^2 + \alpha'_{21}(1-x)^2(2x-1) = 0 \tag{B 4}$$

for a double root. However, from (B 2), if $y = \frac{2}{3}(Z-1)$

$$\tfrac{4}{27}\alpha'_{13}(Z-1) = \alpha'_{21}(1-x)x^2. \tag{B 5}$$

The two equations (B 4) and (B 5) can be solved to give

$$x = 2/(3+Z^{\frac{1}{2}})$$

and

$$\alpha'_{13}/\alpha'_{21} = 27[(3+Z^{\frac{1}{2}})^3(Z^{\frac{1}{2}}-1)]^{-1} \equiv U. \tag{B 6}$$

So when $\alpha'_{13}/\alpha'_{21} = U$ and $y = \frac{2}{3}(Z-1)$, $x = 2/(3+Z^{\frac{1}{2}})$ is a double root. There will also be another solution for x and y when $\alpha'_{13}/\alpha'_{21} = U$, with $F_B^2 < 1$ and $F_T^2 > 1$. Similarly

it can be shown there is a double root for x when $F_B^2 = 1$ (i.e. $x = \frac{2}{3}$). This occurs where

$$y = 2(Z-1)^{\frac{3}{2}}/[Z^{\frac{1}{2}} + 3(Z-1)^{\frac{1}{2}}]$$

and

$$\alpha'_{13}/\alpha'_{21} = \tfrac{1}{27}[3(Z-1)^{\frac{1}{2}} + Z^{\frac{1}{2}}]^3\,[Z^{\frac{1}{2}} + (Z-1)^{\frac{1}{2}}]^{-1}(Z-1)^{-2} \equiv V. \tag{B 7}$$

So for $U < \alpha'_{13}/\alpha'_{21} < V$ there will be three solutions to the equations (B 2) and (B 3) and outside this range there will be only one root.

Appendix C. Stationary Stokes waves in a three-layer system

In this appendix we calculate the amplitudes and wavelengths of stationary waves on an intrusion for which we can put $\partial_t \equiv 0$. The system is as shown in figure 11 with $U_2 = 0$ and with no surface tension forces acting along the interface. The primes on the densities ρ'_1, ρ'_2 and ρ'_3 are dropped. The flow is assumed to be irrotational, so a velocity potential can be defined in each region

$$\phi = U_i x + \phi_i \quad (i = 1, 2, 3). \tag{C 1}$$

The fluid is taken to be incompressible so that

$$\nabla^2 \phi_i = 0 \quad (i = 1, 2, 3). \tag{C 2}$$

The nonlinear kinematic boundary conditions are

$$\left.\begin{aligned} \left(U_1 + \frac{\partial \phi_1}{\partial x}\right)\frac{\partial \eta}{\partial x} = \frac{\partial \phi_1}{\partial z}, \quad \frac{\partial \phi_2}{\partial x}\frac{\partial \eta}{\partial x} = \frac{\partial \phi_2}{\partial z} \quad (z = H_1 + \eta), \\ \left(U_3 + \frac{\partial \phi_3}{\partial x}\right)\frac{\partial h}{\partial x} = \frac{\partial \phi_3}{\partial z}, \quad \frac{\partial \phi_2}{\partial x}\frac{\partial h}{\partial x} = \frac{\partial \phi_2}{\partial z} \quad (z = H_1 + H_2 + h), \end{aligned}\right\} \tag{C 3}$$

$$\frac{\partial \phi_1}{\partial z} = 0 \quad (z = 0), \qquad \frac{\partial \phi_3}{\partial z} = 0 \quad (z = H_1 + H_2 + H_3). \tag{C 4}$$

Continuity of pressure across each interface gives

$$\left.\begin{aligned} \rho_1\left(U_1\frac{\partial \phi_1}{\partial x} + \tfrac{1}{2}(\nabla\phi_1)^2 + g\eta\right) = \rho_2[\tfrac{1}{2}(\nabla\phi_2)^2 + g\eta] \quad (z = H_1 + \eta), \\ \rho_3\left(U_3\frac{\partial \phi_3}{\partial x} + \tfrac{1}{2}(\nabla\phi_3)^2 + gh\right) = \rho_2[\tfrac{1}{2}(\nabla\phi_2)^2 + gh] \quad (z = H_1 + H_2 + h). \end{aligned}\right\} \tag{C 5}$$

The solution to these equations will obviously have $\phi_2 \equiv 0$, as pointed out for a two-layer fluid by Thorpe (1974). The waves on each interface will thus both look like surface waves with a reduced gravity, g'. The waves on the upper and lower interfaces will be completely independent of each other.

Working to third order in the amplitude, a, of the wave, one finds (from Whitham 1974, p. 474) the wavenumber of the stationary mode

$$k = k_0 + a^2 k_1, \tag{C 6}$$

where

$$g' \tanh k_0 H = k_0 U^2$$

and

$$k_1[1 - (2k_0 H/\sinh 2k_0 H)] = \tfrac{1}{8}k_0^3(9\coth^4 k_0 H - 10\coth^2 k_0 H + 9)$$

with $U = U_{1,2}$, $H = H_{1,2}$ and $g' = (\rho_1' - \rho_2')g/\rho_1'$ or $(\rho_3' - \rho_2')g/\rho_3'$ according as one is considering the lower or upper interface.

Equation (C 6) gives the wavelength of the stationary mode in terms of the wave amplitude. In order to calculate the amplitude of the waves the energy flux must be calculated. In a frame moving with the fluid, the energy flux in the waves

$$F' = -\overline{\int_{-H_1}^{\eta} U_1 \rho_1 \left(\frac{\partial \phi_1}{\partial x}\right)^2 dz}.$$

The energy flux in the rest frame will then be given by (Lamb 1932, § 249)

$$F = U_1 E + F', \tag{C 7}$$

where

$$E = \overline{\int_0^{\eta} (\rho_1 - \rho_2) gz\, dz} + \frac{1}{2}\overline{\int_{-H_1}^{\eta} \rho_1 \left[\left(\frac{\partial \phi_1}{\partial x}\right)^2 + \left(\frac{\partial \phi_2}{\partial x}\right)^2\right] dz}.$$

Calculating these integrals and inserting the known values of μ_2, A_1, A_2 and A_4 one obtains

$$\begin{aligned} F = U_1(\rho_1 - \rho_2) ga^2\{\tfrac{1}{4}[1 - (2k_0 H_1/\sinh 2k_0 H_1)] + a^2 k_0^2(\tfrac{9}{64}c^6 - \tfrac{3}{8}c^4 + \tfrac{21}{64}c^2 - \tfrac{9}{32} \\ - k_0 H_1 (\sinh 2k_0 H_1 - 2k_0 H_1)^{-1}[\tfrac{21}{32}c^4 - \tfrac{19}{32}c^2 + \tfrac{9}{16} \\ - k_0 H_1 (\tfrac{21}{16}c^5 - \tfrac{5}{4}c^3 + \tfrac{37}{32}c - \tfrac{9}{16}\tanh k_0 H_1))]\}. \end{aligned} \tag{C 8}$$

So we can now calculate the wavelengths and amplitudes of waves on the lower interface, by setting $F = D_1$. For waves on the upper interface the results are the same but with U_1 replaced by U_3, H_1 by H_3, ρ_1 by ρ_2 and ρ_2 by ρ_3.

REFERENCES

Benjamin, T. B. 1968 Gravity currents and related phenomena. *J. Fluid Mech.* **31**, 209.

Benjamin, T. B. 1966 Internal waves of finite amplitude and permanent form. *J. Fluid Mech.* **25**, 241.

Britter, R. E. & Simpson, J. E. 1978 Experiments on the dynamics of a gravity current head. *J. Fluid Mech.* **88**, 223.

Burnside, W. S. & Panton, A. W. 1960 *The Theory of Equations*. Dover.

Cokelet, E. D. 1977 Steep gravity waves in water of arbitrary depth. *Phil. Trans. Roy. Soc.* A **286**, 183.

Gardner, G. C. & Crow, I. G. 1970 The motion of large bubbles in horizontal channels. *J. Fluid Mech.* **43**, 247.

Kármán, T. von 1940 The engineer grapples with nonlinear problems. *Bull. Am. Math. Soc.* **46**, 615.

KEULEGAN, G. H. 1958 The motion of saline fronts in still water. *Nat. Bur. Stand. Rep.* 5831.

LAMB, H. 1932 *Hydrodynamics*. Cambridge University Press.

LIGHTHILL, M. J. 1978 *Waves in Fluids*. Cambridge University Press.

PHILLIPS, O. M. 1977 *The Dynamics of the Upper Ocean*. Cambridge University Press.

SALMON, G. 1866 *Lessons on Higher Algebra*, 2nd ed. Dublin.

SIMPSON, J. E. 1969 A comparison between laboratory and atmospheric density currents. *Q. Jl Meteor. Soc.* **95**, 758.

STOKES, G. G. 1880 Considerations relative to the greatest height of oscillatory irrotational waves. *Math. and Phys. Papers*, vol. 1, p. 225. Cambridge University Press.

THORPE, S. A. 1974 Near resonant forcing in a shallow two-layer fluid: a model for the internal surge in Loch Ness? *J. Fluid Mech.* **63**, 509.

WHITHAM, G. B. 1974 *Linear and Non-linear Waves*. Wiley.

ZUKOVSKI, E. E. 1966 Influence of viscosity, surface tensions, and inclination angle on motion of long bubbles in closed tubes. *J. Fluid Mech.* **25**, 821.

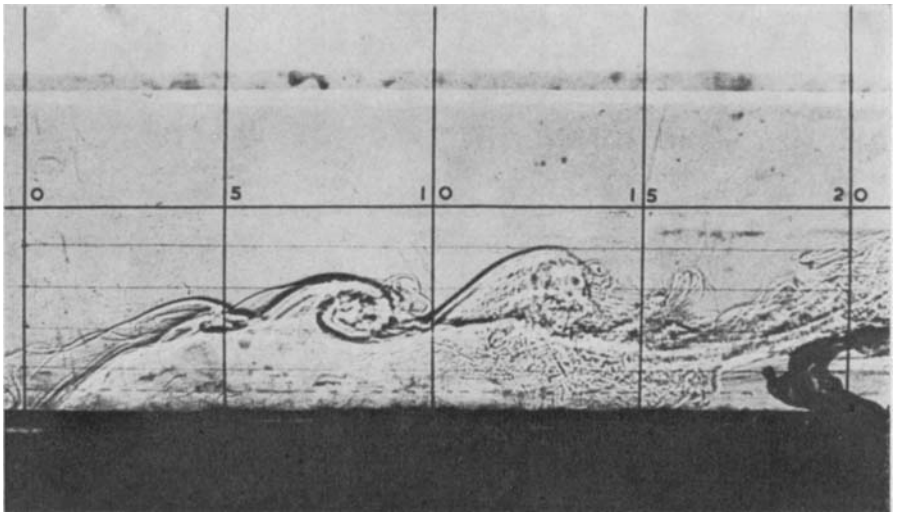

FIGURE 1. Kelvin–Helmholtz billows on a boundary current.
For the experimental details, see Britter & Simpson (1978).

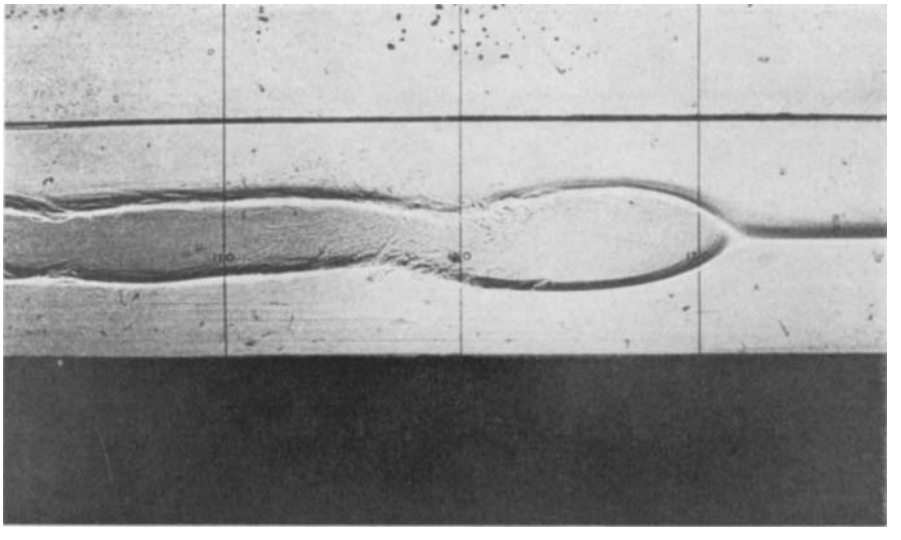

FIGURE 12. An intrusion with $Z = 2$ and $\alpha'_{21} = 1{\cdot}48 \times 10^{-2}$ and $\alpha'_{13} = 1{\cdot}52 \times 10^{-2}$.

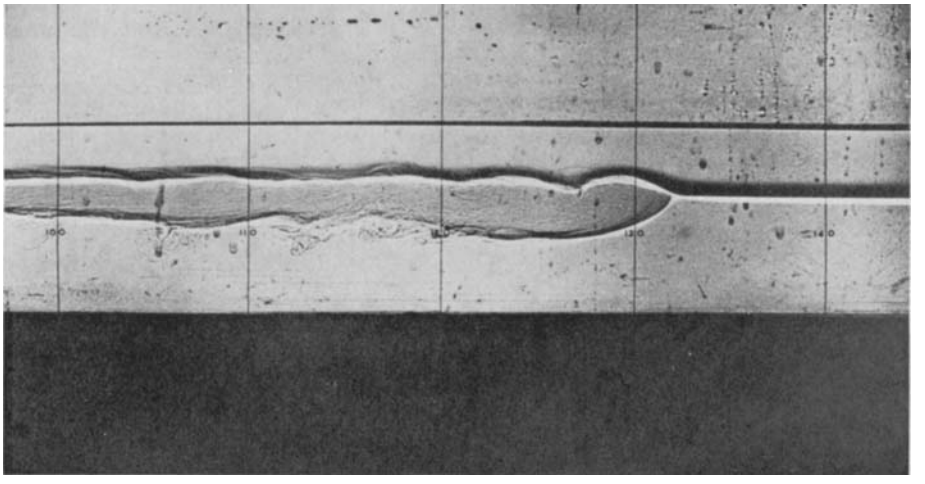

FIGURE 13. An intrusion with $Z = 1{\cdot}5$ and $\alpha'_{21} = 4{\cdot}49 \times 10^{-3}$ and $\alpha'_{13} = 1{\cdot}01 \times 10^{-2}$.

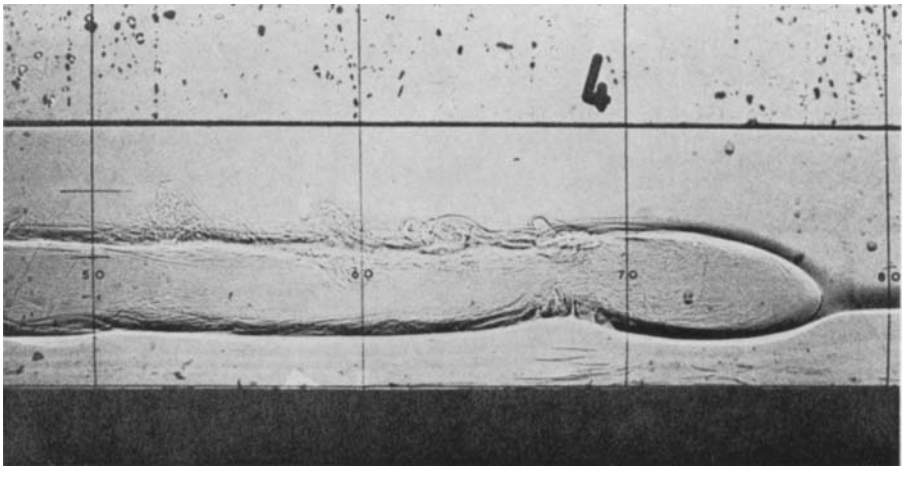

FIGURE 14. An intrusion with $Z = 3$ and $\alpha'_{21} = 1{\cdot}97 \times 10^{-2}$ and $\alpha'_{13} = 1{\cdot}01 \times 10^{-2}$.